8 Stratified 2D Flows

This note illustrates some basic phenomena of stratified flows computed with Nek5000 using a Boussinesq approximation. We consider a two-dimensional flow with free-stream velocity U past a cylinder of diameter D and examine blocking, the Brünt-Väsäillä frequency, and the wave-like nature of stratified flow. Our discussion closely follows the introductory material given by Tritton.[11]

We assume that the density of the fluid is given by $\rho = \rho_0 + \rho'(\mathbf{x}, t)$, where the background density $\rho_0 \gg \rho'$ is constant. To first order, the perturbation ρ' only acts through the gravitational forcing in the momentum equations, given in dimensional form by

$$\rho_0 \left(\frac{\partial \mathbf{u}}{\partial t} + \mathbf{u} \cdot \nabla \mathbf{u} \right) = -\nabla p + \rho_0 \nu \nabla^2 \mathbf{u} - g \left(\rho_0 + \rho' \right) \hat{\mathbf{y}}. \tag{9}$$

The constant $-g\rho_0\hat{\mathbf{y}}$ can be absorbed into the pressure (as can any other potential field), so the dynamical influence of the stratification is driven only by the perturbation density ρ'. In addition to (9), we have the standard incompressibility constraint

$$\nabla \cdot \mathbf{u} = 0, \tag{10}$$

and the transport equation

$$\frac{\partial \rho'}{\partial t} + \mathbf{u} \cdot \nabla \rho' = \kappa \nabla^2 \rho', \tag{11}$$

which reflects the fact that the density perturbation is tied to a scalar quantity, such as salinity or temperature, that satisfies a convection-diffusion equation. (Note that Nek5000 readily handles a variable ρ_0 as well. The current studies, however, follow the formulation given by (9)–(11).)

We assume a linear profile for the initial condition of (11). That is,

$$\rho'_{y,0} := \left. \frac{\partial \rho'}{\partial y} \right|_{t=0} = constant.$$

Under these circumstances, there is an intrinsic timescale associated the stratification, which is usually expressed by its inverse, namely, the Brünt-Väsäillä frequency:

$$N_{BV} := \left(\frac{g}{\rho_0} {\rho'}_{y,0} \right)^{\frac{1}{2}}. \tag{12}$$

We return to this in the discussion below but introduce it here, prior to nondimensionalization, to stress that it is independent of any timescale associated with the external flow.

Before proceeding with the examples, we rescale the governing system of equations by the length scale D and convective timescale D/U to arrive at the nondimensional system

$$\frac{\partial \mathbf{u}}{\partial t} + \mathbf{u} \cdot \nabla \mathbf{u} = -\nabla p + \frac{1}{Re} \nabla^2 \mathbf{u} - \frac{1}{Fr^2} (\rho' - y) \hat{\mathbf{y}} \tag{13}$$

$$\nabla \cdot \mathbf{u} = 0 \tag{14}$$

$$\frac{\partial \rho'}{\partial t} + \mathbf{u} \cdot \nabla \rho' = \frac{1}{PrRe} \nabla^2 \rho'. \tag{15}$$

Here, we have slightly abused the notation by using the same symbols for the dimensional and nondimensional variables; there will be no confusion, however, given the context in which each

[11] D.J. Tritton, *Physical Fluid Dynamics*, Oxford (1988).

is used. In addition to rescaling, we divided (9) and normalized the pressure by ρ_0, and have introduced three nondimensional parameters,

$$Re = \frac{UD}{\nu}, \qquad Pr = \frac{\kappa}{\nu}, \qquad Fr^{-2} = \frac{gD^2}{\rho_0 U^2} \left|\rho'_{y,0}\right|, \tag{16}$$

which are, respectively, the Reynolds number, the Prandtl (or Schmidt) number, and the Froude number. Note that the it is common to replace the Froude number by the Richardson number, $Ri := Fr^{-2}$. Finally, we have introduced an additional potential,

$$-\frac{1}{Fr^2} y\hat{\mathbf{y}}, \tag{17}$$

to remove the hydrostatic mode (associated with ρ') from the pressure.

We have computed steady-state flow past a cylinder at $Re = 10$ using the two-dimensional mesh shown in Fig. 7(a). The mesh comprises $E = 346$ elements of order $N = 7$. A uniform inflow of speed $U = 1$ is specified at the left boundary and symmetry conditions are specified on the top and bottom boundaries. The Neumann (natural) condition for the Stokes problem,

$$\frac{\partial u_i}{\partial n} + p = 0, \quad i = 1, 2,$$

is applied on the right boundary, which effectively corresponds to having $p = 0$ at the outflow. It is for this reason that we use (17) to remove the hydrostatic contribution to the pressure.

The solutions are time-marched to steady state. The initial condition for the unstratified case of Fig. 7(a) was $\mathbf{u} = (1, 0, 0)$. The converged steady-state velocity field of (a) was used as the initial condition for the stratified cases (b) and (c). the initial density profiles were $\rho' = -y$. (The cylinder is centered at $(0, 0)$.)

8.1 Steady State Results

Figures 7(b)–(d) show steady-state streamline patterns under different stratification conditions. Case (b) is standard Navier-Stokes flow without stratification. It exhibits a classic wake structure with flow separation at roughly 29 degrees from the horizontal axis and a small recirculation zone of length $\approx D/4$ aft of the cylinder.

The streamline patterns in Fig. 7(c) and (d) are in marked contrast to those in (b). In Fig. 7(c), we see that there are wakes both in front and behind the cylinder, while in (d) there is a wake only in front of the cylinder. In (c) and (d), the Froude number is $Fr = 1000^{1/2}$, which corresponds to significant stratification. This results in a phenomenon known as *blocking*, which occurs when the dynamic head of the fluid is insufficient to overcome the potential energy barrier associated with climbing above (or descending below) the cylinder. Fluid particles are essentially trapped at a given height. As explained in Tritton, the length of the forward wake is determined by viscous effects, and scales as $O(Re/Fr^2)$, provided the domain is sufficiently large.

While the flow upstream of the cylinder in Figs. 7(c) and (d) is similar in structure, the downstream behavior is decidely different. The flow conditions in (c) and (d) are identical, save that $Pr = 1$ in (c) and $Pr = 1000$ in (d). The change in the flow behavior can be explained as follows. Through density diffusion, a fluid parcel that flows close to the cylinder in case (c) takes on the local density by the time it reaches the cylinder apex. As it passes the cylinder, it has a tendency to remain at its new height and thus only slowly returns to its original height, resulting in an extended wake. For large Pr, however, the density diffusion is small. A particle passing the cylinder thus retains its original density and quickly returns to its original height after passing the cylinder. This results in the streamline pattern of Fig. 7(d). (Note that the Schmidt number for salt water is $Sc \approx 700$, so $Pr = 1000$ is not far from being physically realizable.)

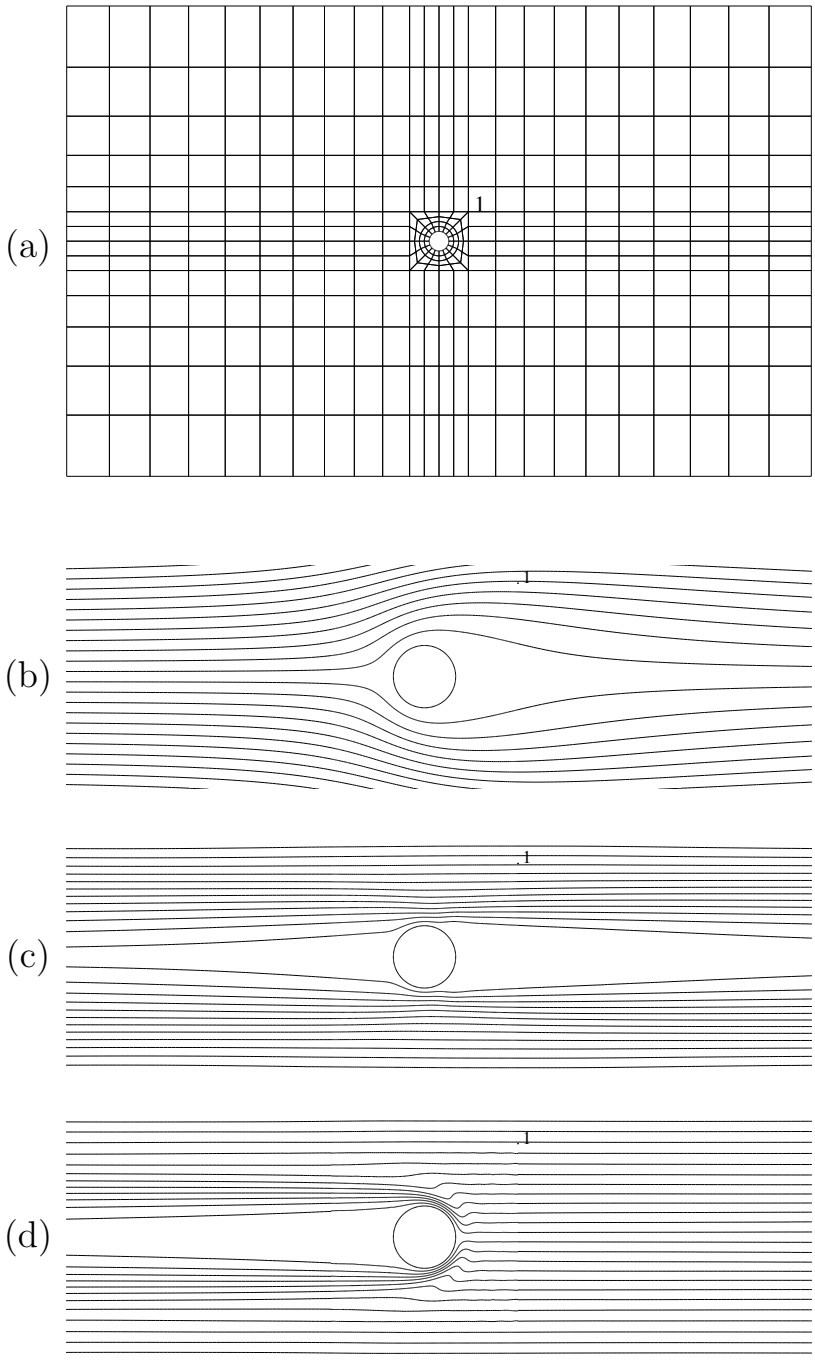

Figure 7: Examples of blocking phenomena in stratified flow at $Re = 10$: (a) spectral element mesh, (E, N)=(384, 7), and steady-state streamfunction distribution for (b) no stratification, (c) Fr^{-2}=1000, $Pr = 1$, and (d) Fr^{-2}=1000, $Pr = 1000$.

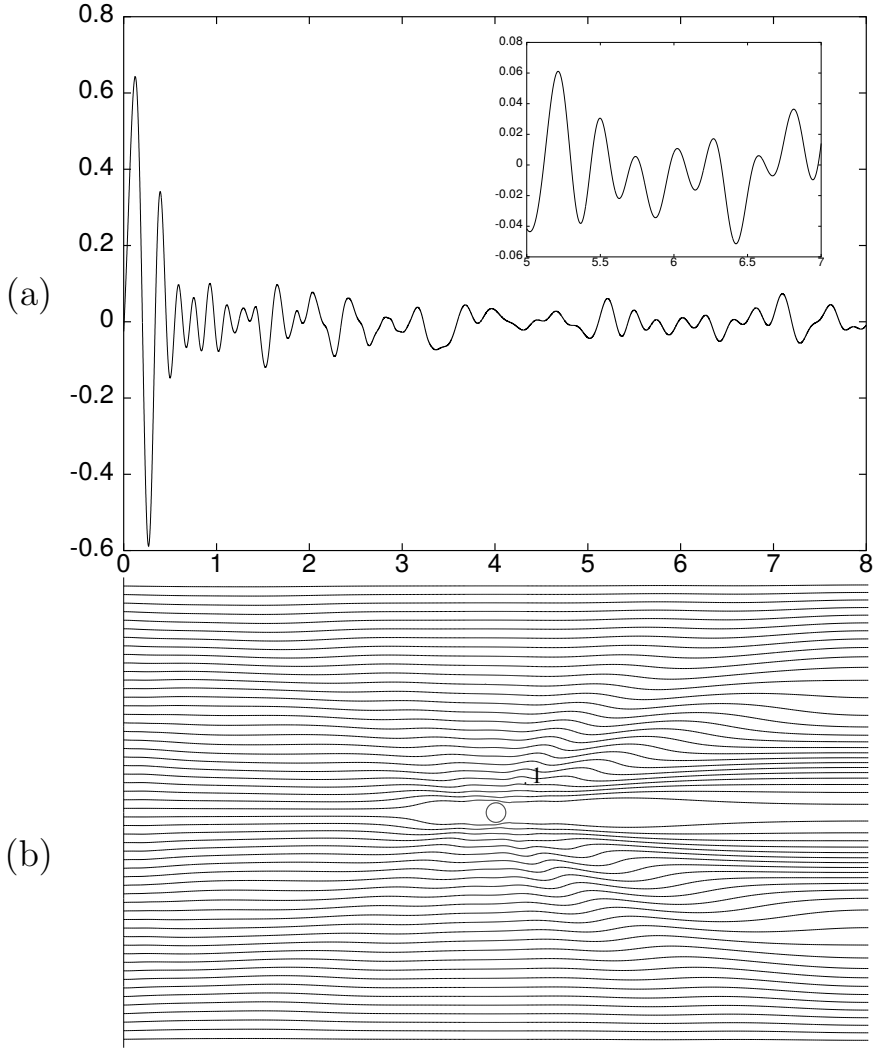

Figure 8: Wave-like response to sudden application of gravitation forcing for Fr^{-2}=1000, Pr = 1000: (a) time trace of v at point "1" indicated in (b); (b) instantaneous streamline pattern at $t = 0.5$.

8.2 Unsteady Results

In addition to the steady phenomena depicted in Fig. 7, two-dimensional stratified flows exhibit interesting dynamical behavior. Under the high loading implied by a small Froude number, one can expect timescales that are significantly shorter than the convective timescale of classic incompressible flow. To illustrate, we consider the following simplified model of stratified flow. Assume that a fluid parcel with volume V is displaced a distance Δy in a body of fluid that is otherwise at rest. The restoring force is proportional to the volume of the fluid, the difference between its density and the surrounding fluid, and the gravitational constant, g. In dimensional units, we have

$$F = -V(\frac{\partial \rho}{\partial y}\Delta y)g.$$

This force accelerates the parcel in a direction opposite to Δy, resulting in the equation of motion

$$\frac{d^2\Delta y}{dt^2} + \left(\frac{g}{\rho}\frac{\partial \rho}{\partial y}\right)\Delta y = 0,$$

which obviously leads to simple harmonic motion with frequency

$$N_{BV} := \sqrt{\frac{g}{\rho}\frac{\partial \rho}{\partial y}}.$$

Because U=1 and D=1 in the current nondimensionalization, we have from (16) $N_{BV} = Ri^{\frac{1}{2}} = Fr^{-1}$, with corresponding period $\tau_{BV} = 2\pi Fr$.

Figure 8(a) shows the history of the vertical velocity component at the point indicated by the "1" in Fig. 8(b). The initial conditions for $\mathbf{u}$ and ρ' are taken to be the steady-state flow conditions of Fig. 7(b), with Pr=1000. When the forcing is turned on, the density distribution is far from equilibrium and oscillations ensue. The oscillations in the inset in Fig. 8(a) correspond to a period of $\tau \approx 0.257$, in close agreement with $\tau_{BV} = .199$. That $\tau > \tau_{BV}$ can be understood by the fact that, because of incompressibility and the boundary conditions, the vertical displacement of any given fluid parcel must be associated with the horizontal displacement of some other parcels that add mass to the displaced system but do not add potential energy. As a consequence, the frequency will be lowered.

Tritton carries the unsteady analysis further and points out that disturbances in stably stratified flows can propagate as waves. Wave patterns are clearly evident in Fig. 8(b), which shows the instantaneous streamlines at time $t = 0.5$ for the flow associated with Fig. 8(a). Note that this convective time corresponds to the time it takes a particle in the free stream to move half a diameter. However, the wake structures and multiple waves can be seen to extend *several* diameters away from from the cylinder at this early time. We note that the loading is applied instantaneously *throughout* the domain, and that the nonequilibrium displacement of ρ' at $t = 0$ may already extend several diameters in the initial conditions.) Nonetheless, it is clear from Fig. 8(b) and other similar early-time images that information is propagating on a timescale that is much shorter than the convective timescale.

Tritton also derives a dispersion relationship for the wave phenomenon that gives the frequency as a function of the vectorial wave number

$$\omega = N_{BV} \sin\theta,$$

where θ is the angle of the wave vector with respect to the vertical axis. From the preceding estimates of τ, we can estimate the angle of the wave vector to be ≈ 50.6 degrees, which is in reasonable agreement with the pattern observed near history point "1" in Fig. 8(b).

8.3 Implications for Simulation

We close with a few numerical considerations encountered in these simulations.

First, because the bouyancy force is treated explicitly in Nek5000 and because it is associated with a fast timescale (for small Fr), the timestep size will generally be much less than the usual Courant-limited timestep.

Second, it is important to respect $p = 0$ at the outflow boundary, as much as possible. Also, it is important to start the simulation close to equilibrium. Otherwise, the wave motions can suck fluid in through the outflow boundary, which is usually disastrous.

Third, the wavelike nature of stratified flow implies a potential need for radiation boundary conditions, if significant wave energy is to leave the domain through an artificial domain boundary.

Fourth, we note that N_{BV} is based upon the vertical density gradient. In the case of a sharp interface, with densities ρ_1' and ρ_2' on either side, it should be redefined in terms of the density jump $\rho_2' - \rho_1'$.

Fifth, turbulence, if present, will generally yield an order-unity (effective) Prandtl/Schmidt number.